

Scanning tunneling microscopy and spectroscopy of arsenic antisites in low temperature grown InGaAs

B. Grandidier, Huajie Chen, and R. M. Feenstra

Department of Physics, Carnegie Mellon University, Pittsburgh, Pennsylvania
15213

D. T. McInturff

School of Electrical and Computer Engineering, Purdue University, West
Lafayette, Indiana 47907

P. W. Juodawlkis and S. E. Ralph

School of Electrical and Computer Engineering, Georgia Institute of Technology,
Atlanta, Georgia 30322-0250

Abstract

Scanning tunneling microscopy is used to study low temperature grown (LTG) InGaAs, with and without Be doping. The Be-doped material is observed to contain significantly fewer As_{Ga} antisite defects than the undoped material, with no evidence found for Be-As complexes. Annealing of the LTG-InGaAs forms precipitates preferentially in the undoped material. The previously observed dependence of the optical response time on Be-doping and annealing is attributed to changes in the As antisite concentration and the compensation effect of the Be.

Low temperature grown (LTG) III-V semiconductor materials are known to contain excess arsenic. This change in the stoichiometry leads to several interesting properties such as a fast absorption recovery time or a high resistivity when the materials are subsequently annealed. Although most of the LTG semiconductor materials studies to date have been performed on GaAs, the possibility of producing devices having a subpicosecond return to equilibrium dynamic in the 1.55 μm wavelength region has produced a growing interest in LTG-InGaAs and InGaAs/InAlAs multiquantum well structures.[1,2] Compared to LTG-GaAs, the concentration of As-based deep centers is smaller in LTG-InGaAs,[3] resulting in a longer absorption recovery time in undoped material.[4] When LTG-InGaAs is doped with beryllium, the photoexcited free-carrier lifetime becomes shorter and comparable to that of LTG-GaAs (subpicosecond electron lifetimes have been observed [5]). Whereas annealing of undoped material is found to dramatically slow the absorption recovery time,[6] Be doping maintains the fast recovery time. To explain this effect, the presence of midgap states has been proposed, arising from complexes between Be dopants and the excess As introduced during growth.[1,2,4,5] The direct compensation effect of the Be has also been suggested.[4]

In this work, we report a study of undoped and Be-doped LTG-InGaAs layers by scanning tunneling microscopy and spectroscopy. The scanning tunneling microscope (STM) has been previously used to observe defects in LTG-GaAs.[6] As for that case, we observe in LTG-InGaAs the presence of arsenic antisites. We find a significantly lower concentration of antisites in the as-grown Be-doped material compared to the undoped material (with the difference being much great-

er than the Be concentration). An observed shift in Fermi-level position resulting from this decreased antisite concentration provides an explanation for the greatly reduced carrier concentration in the Be-doped case.[5] After annealing at 600° C, precipitates are found to form in the undoped material, but not for the Be-doped case. The difference in photoresponse time between the undoped and Be-doped annealed LTG-InGaAs is thus attributed to a lower As point defect density in the undoped case (the precipitates, which are small and widely spaced, act as slow recombination centers [7]). Be-As complexes have not been detected, neither in as-grown nor annealed material.

The 1µm thick LTG-In_{0.53}Ga_{0.47}As layers were grown at 240° C by molecular beam epitaxy on a 100 nm n-type In_{0.53}Ga_{0.47}As buffer layer, on an InP substrate. We discuss two samples: one undoped and the other with a Be doping concentration of $2 \times 10^{18} \text{ cm}^{-3}$ in the LTG layer. Portions of the samples were annealed at 600° C for 30 s. The samples were cleaved in an STM ultra-high vacuum chamber with a base pressure $< 5 \times 10^{-11}$ Torr, and the exposed (1 $\bar{1}$ 0) face was immediately examined with the STM in the same chamber. Polycrystalline W tips were chemically etched, and cleaned *in-situ* by electron bombardment. STM images were obtained with a constant tunnel current of 0.1 nA, and at sample voltages specified below. For all the spectroscopic measurements the tip-sample separation is varied as the voltage is scanned according to $\Delta s = -a |V|$ with $a \approx 1.3 \text{ \AA/V}$. Normalization of the spectra is performed as described in Ref. 8.

Figure 1(a) shows a constant current image of the Be-doped LTG-InGaAs layer. This high-resolution image is acquired with a negative sample bias, so that the background atomic corrugation arises from the As-sublattice of the In_{0.53}Ga_{0.47}As layer. Depending on the cation neighbors of a particular As surface atom, the contrast of the arsenic atoms varies [9] and this explains why the As-sublattice of the (1 $\bar{1}$ 0) InGaAs surface does not appear homogeneous. Near the center of Fig. 1(a), a bright protrusion superimposed to the As-sublattice is clearly visible. This defect is also seen in the associated conductance image, Fig. 1(b), where it appears dark. In both images, the defect is characterized by a central core and two satellites peaks along the [112] and [$\bar{1}\bar{1}$ 2] directions. This defect is similar to the defects already characterized in LTG-GaAs and is identified as an arsenic antisite, As_{Ga} . According to its symmetry, it belongs to the second layer (*i.e.* one layer below the surface).[6,10]

Figures 1(c) and (d) contain STM images taken from the Be-doped LTG-InGaAs sample and the undoped LTG-InGaAs sample respectively. Figure 1(c) is a current image, obtained by imaging at constant current using a voltage outside the band gap and then, at each pixel, opening the feedback loop and recording the current at a voltage near the edge of the valence band, -0.85 V in this case. Figure 1(d) is a constant current image acquired at a sample voltage of -1.0 V, corresponding to an energy close to the valence band edge. In both images, defects are visible. Some are similar to the one seen in Fig. 1(a), and others appear with varying size and brightness. According to the previous work on LTG-GaAs, all these defects are associated with arsenic antisites belonging to different atomic layers.[6] A comparison between Figs. 1(c) and (d) reveals a higher concentration of antisites in the undoped layer, with 8 antisites visible in Fig. 1(c) and 24 in Fig. 1(d). Counting antisites in all our images, obtained on several pieces of the samples using different probe tips, we get concentrations of $(30 \pm 5) \times 10^{18} \text{ cm}^{-3}$ for the undoped LTG-InGaAs layer and $(7.0 \pm$

$1.5) \times 10^{18} \text{ cm}^{-3}$ for the Be-doped material. The antisite concentration thus seems to be lower in LTG-InGaAs than in LTG-GaAs samples where a concentration of $1 \times 10^{20} \text{ cm}^{-3}$ is usually found for a growth temperature of 220°C , [6] close to that used for our samples. This result is in agreement with the reduced antisite concentration previously found in electrical studies of LTG-InGaAs, [3,11] for which a possible explanation is a smaller sticking coefficient of As atoms on InGaAs compared to pure GaAs. [12] Comparing the antisite concentration between the undoped and the Be-doped layers, a ratio of 4.3 is obtained. A similar ratio was also found in LTG-GaAs grown at 250°C , although the Be concentration, $1 \times 10^{19} \text{ cm}^{-3}$, was higher in that case. [13]

Annealing studies for the Be-doped material are shown in Figs. 2(a) and (b). No precipitates were observed, although individual antisites with their characteristic satellite features are well resolved in the filled-state image of Fig. 2(a). The simultaneously acquired empty-state image, Fig. 2(b), displays bright protrusions at the position of the antisites. After annealing, the concentration of As_{Ga} is $(5.0 \pm 1.5) \times 10^{18} \text{ cm}^{-3}$, nearly the same as the As_{Ga} concentration prior to annealing. The voltage dependence of the antisites contrasts with that of the Be impurities, denoted Be in Fig. 2(b). The Be dopants, being acceptor impurities in n-type material, appear as bright hillocks in the filled state image and as depressions in the empty state image. We observe varying brightness for the hillocks in the filled state image, corresponding to different positions of the impurities under the $(1\bar{1}0)$ surface. Using a typical discernable depth for dopants of four atomic layers, [14] we find a Be impurity concentration of $(2.1 \pm 0.2) \times 10^{18} \text{ cm}^{-3}$, in good agreement with the intended dopant concentration. For the case of the undoped material, we find that annealing reduces the antisite concentration by a factor of five, to $(6.0 \pm 1.5) \times 10^{18} \text{ cm}^{-3}$. Small clusters, consisting presumably of arsenic precipitates, are also observed, with typical diameter of 75 \AA and number density of about $1 \times 10^{16} \text{ cm}^{-3}$. We thus conclude that our 30 s, 600°C anneal is sufficient to initiate the precipitate formation in the undoped material, in agreement with the results of Ibbettson *et al.* [11] In addition, we find that the tendency to form precipitates is significantly diminished in the Be-doped material, which is also in good agreement with past studies on LTG-GaAs. [15]

Information on the electronic properties of the LTG-InGaAs is obtained from STM spectroscopic measurements, as shown in Fig. 3. Spectra (a) and (b) were measured on the undoped, as-grown LTG-InGaAs layer, whereas spectrum (c) was acquired on the Be-doped as-grown material. Spectra (d) and (e) were obtained after annealing the undoped and Be-doped samples respectively. Band edges are clearly resolved in the spectra and are marked by dotted lines. Within an experimental uncertainty of $\pm 0.07 \text{ eV}$, the measured gaps equal the known value of 0.75 eV . Spectrum (a) was obtained by positioning the tip on a second layer As antisite, like the one displayed in Fig. 1(a). It reveals an intense band of midgap states, centered at $E_C - 0.15 \text{ eV}$, similar to that observed in LTG-GaAs. [6] For antisites in $\text{In}_{0.53}\text{Ga}_{0.47}\text{As}$, an energy level has been observed at $E_C - 0.032 \text{ eV}$, [3] which we associate with the first donor level (0/+). In analogy with GaAs, [16] a second donor level (+/++) is expected 0.23 eV below that. The band of states observed in spectrum (a) near $E_C - 0.15 \text{ eV}$ we attribute of a combination of these states, with some additional broadening produced by Coulomb interactions between neighboring antisites. The shoulder at $E_C - 0.5 \text{ eV}$ in spectrum (a) we attribute to the free carrier component of the conductance (identical to the “dopant-induced” component seen in doped GaAs [6]). A similar component is seen in spectrum

(b), observed far from an antisite defect, thus providing strong evidence of a large concentration of free electrons in this material. In the undoped material, spectra (a) and (b), the Fermi-level (0 V) is located at $E_C + (0.05 \pm 0.05)$ eV. Spectrum (c) was acquired from the Be-doped layer, with the tip far from any antisite defects. Here, the Fermi-level is located at $E_C - (0.07 \pm 0.05)$ eV. Calculations of electron occupation, using the concentrations and energy levels given above, indicate that this observed Fermi-level shift between undoped and Be-doped material is consistent with the drop in residual carrier concentration observed between these materials.[5] Finally, spectra (d) and (e), obtained from annealed material with the tip positioned far from any defects, show similar Fermi-level positions as (b) and (c) respectively.

For both undoped and Be-doped samples, we could not detect any other defects with a concentration comparable to that of the antisites, aside from the presence of surface vacancies which are well known on cleaved III-V surfaces. In particular, we find no evidence for $Be_{Ga}-As_{Ga}$ pairs. Since the concentration of complexes between Be dopants and As antisites is apparently small, we consider it unlikely that these defects are responsible for the reported photoexcited carrier lifetime shortening in LTG-InGaAs:Be samples.[4,5] Instead, our data supports a model based on the difference in Fermi-level position between undoped and Be-doped material. Furthermore, we establish that the preferential formation kinetics for precipitates in the undoped material, together with the compensation effect of Be, can explain the observed data. The significantly lower Fermi-level position observed in Be-doped material will lead to a larger concentration of ionized antisites, As_{Ga}^+ , and a faster photoresponse. Therefore, for as-grown material, Be-doping leads to fewer antisites but this is more than offset by the compensation effects of the Be, so that a greater fraction of the antisites are ionized. The photoresponse is thus faster than for undoped material. After annealing, the undoped material experiences a sharp drop in antisite concentration, and few of these remaining defects are ionized. Precipitates are present, but they behave as slow recombination centers. Thus, the annealed undoped material has a slow photoresponse time, whereas the annealed Be-doped material maintains its fast response.

In conclusion, we have used the STM to observe arsenic-related point defects in LTG-InGaAs. These defects have the same geometric and electronic properties as the defects found in LTG-GaAs, and thus we identify them as arsenic antisites. A comparison between undoped and Be-doped LTG-InGaAs layers shows a decrease of the antisite concentration for the Be-doped sample. The cause of this decrease is not understood, although it may be caused by a higher incorporation rate on Ga sites of Be impurities in comparison to As during the growth, as already mentioned by Missous and others.[13,17] No other defect with midgap states and a concentration comparable to the As_{Ga} concentration has been found. After annealing, precipitates are observed in the undoped material but not for the Be-doped case. The reduced photoresponse time observed for the annealed, undoped material is thus attributed to the presence of the precipitates, which are believed to act as slow recombination centers.

This work was supported by the National Science Foundation under grant DMR-9615647, and the MRSEC program under grant 9400415-0144.

- [1] R. A. Metzger, A. S. Brown, L. G. McCray, and J. A. Henige, *J. Vac. Sci. Technol. B* **11**, 798 (1993).
- [2] R. Takahashi, Y. Kawamura, T. Kagawa, and H. Iwamura, *Appl. Phys. Lett.* **65**, 1790 (1994).

- [3] H. Künzel, J. Böttcher, R. Gibis, and G. Urmann, *Appl. Phys. Lett.* **61**, 1347 (1992).
- [4] P. W. Juodawlkis, D. T. McInturff, and S. E. Ralph, *Appl. Phys. Lett.* **69**, 4062 (1996).
- [5] Y. Chen, S. S. Prabhu, S. E. Ralph, and D. T. McInturff, *Appl. Phys. Lett.* **72**, 439 (1998).
- [6] R. M. Feenstra, J. M. Woodall, and G. D. Pettit, *Phys. Rev. Lett.* **71**, 1176 (1993); *Mat. Sci. Forum* **143-147**, 1311 (1994).
- [7] E. S. Harmon, M. R. Melloch, J. M. Woodall, D. D. Nolte, N. Otsuka, and C. L. Chang, *Appl. Phys. Lett.* **63**, 2248 (1993).
- [8] P. Mårtensson and R. M. Feenstra, *Phys. Rev. B* **39**, 7744 (1988); R. M. Feenstra, *Phys. Rev. B* **50**, 4561 (1994).
- [9] M. Pfister, M. B. Johnson, S. F. Alvarado, H. W. M. Salemink, U. Marti, D. Martin, F. Morier-Genoud, and F. K. Reinhart, *Appl. Phys. Lett.* **67**, 1459 (1995).
- [10] R. B. Capaz, K. Cho, and J. D. Joannopoulos, *Phys. Rev. Lett.* **75**, 1811 (1995).
- [11] J. P. Ibbetson, J. S. Speck, A. C. Gossard, and U. K. Mishra, *Appl. Phys. Lett.* **62**, 2209 (1993).
- [12] S. Y. Karpov and M. A. Maiorov, *Surf. Sci.* **344**, 11 (1995).
- [13] R. E. Pritchard, S. A. McQuaid, L. Hart, R. C. Newman, J. Mäkinen, H. J. von Bardeleben, and M. Missous, *J. Appl. Phys.* **78**, 2411 (1995).
- [14] M. B. Johnson, O. Albrechtsen, R. M. Feenstra, and H. W. M. Salemink, *Appl. Phys. Lett.* **63**, 2923 (1993); **64**, 1454 (1994).
- [15] M. R. Melloch, N. Otsuka, K. Mahalingam, C. L. Chang, P. D. Kirchner, J. M. Woodall, and A. C. Warren, *Appl. Phys. Lett.* **61**, 177 (1992); *J. Appl. Phys.* **72**, 3509 (1992).
- [16] E. R. Weber, H. Ennen, U. Kaufman, J. Windscheif, J. Schneider, and T. Wosinski, *J. Appl. Phys.* **53**, 6140 (1982).
- [17] S. P. O'Hagan and M. Missous, *Compound Semiconductor Epitaxy Symposium*, p. xv+612, 295-300 (1994).

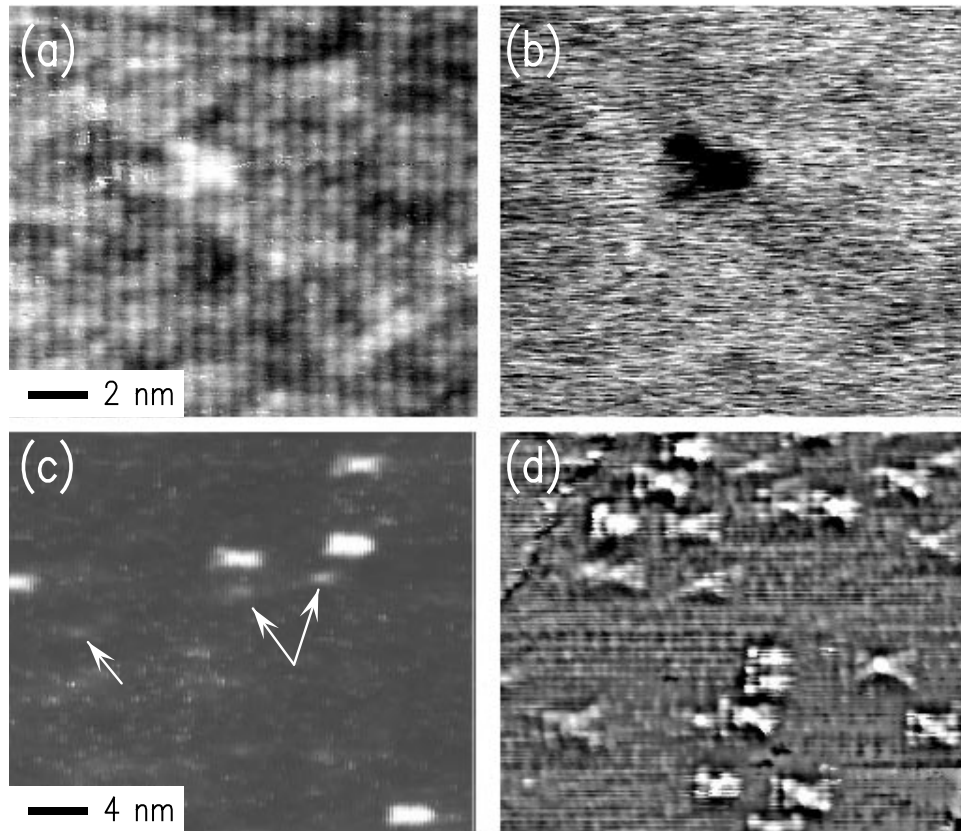


Figure 1 (a) Constant current image and (b) associated conductance image of the $(1\bar{1}0)$ cleaved surface of Be-doped LTG-InGaAs, acquired with 0.1 nA tunnel current, at a sample bias of -1.45 V. A point defect with two satellites features is observed in both images. The grey scale range in (a) is 0.8 Å. (c) Current image of the Be-doped LTG-InGaAs sample and (d) constant current image of the undoped LTG-InGaAs sample. The images were acquired at sample voltages of (c) -0.85 V and (d) -1.00 V. A local background subtraction has been performed in (d) to enhance the contrast in the image. Various point defects (arsenic antisites) can be seen. In (c), the deeper subsurface point defects are indicated by arrows.

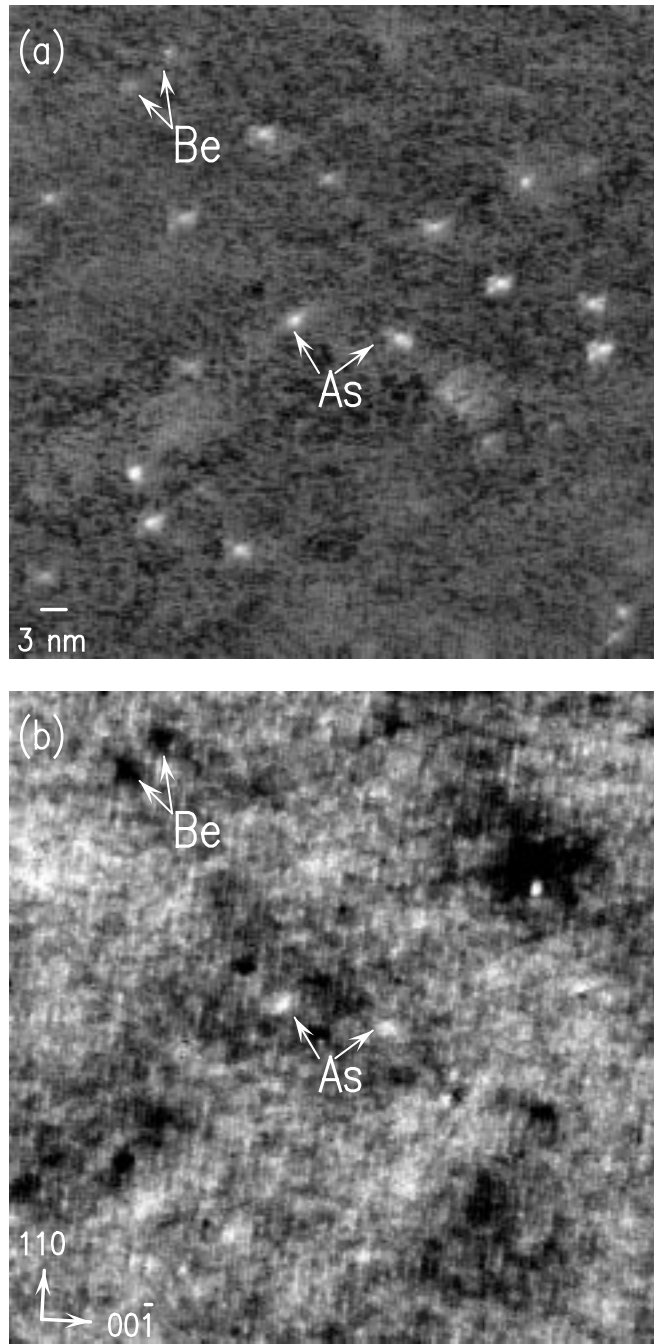


Figure 2 STM images of a cleaved Be-doped LTG-InGaAs sample after annealing at 600°C for 30 s. Both images were acquired simultaneously at sample voltages of (a) -1.45 V and (b) $+1.25\text{ V}$. Grey scale ranges are (a) 4.8 \AA and (b) 1.6 \AA . Several dopants and antisites are seen. Two Be impurities (Be) and two arsenic antisites (As) are indicated on the images.

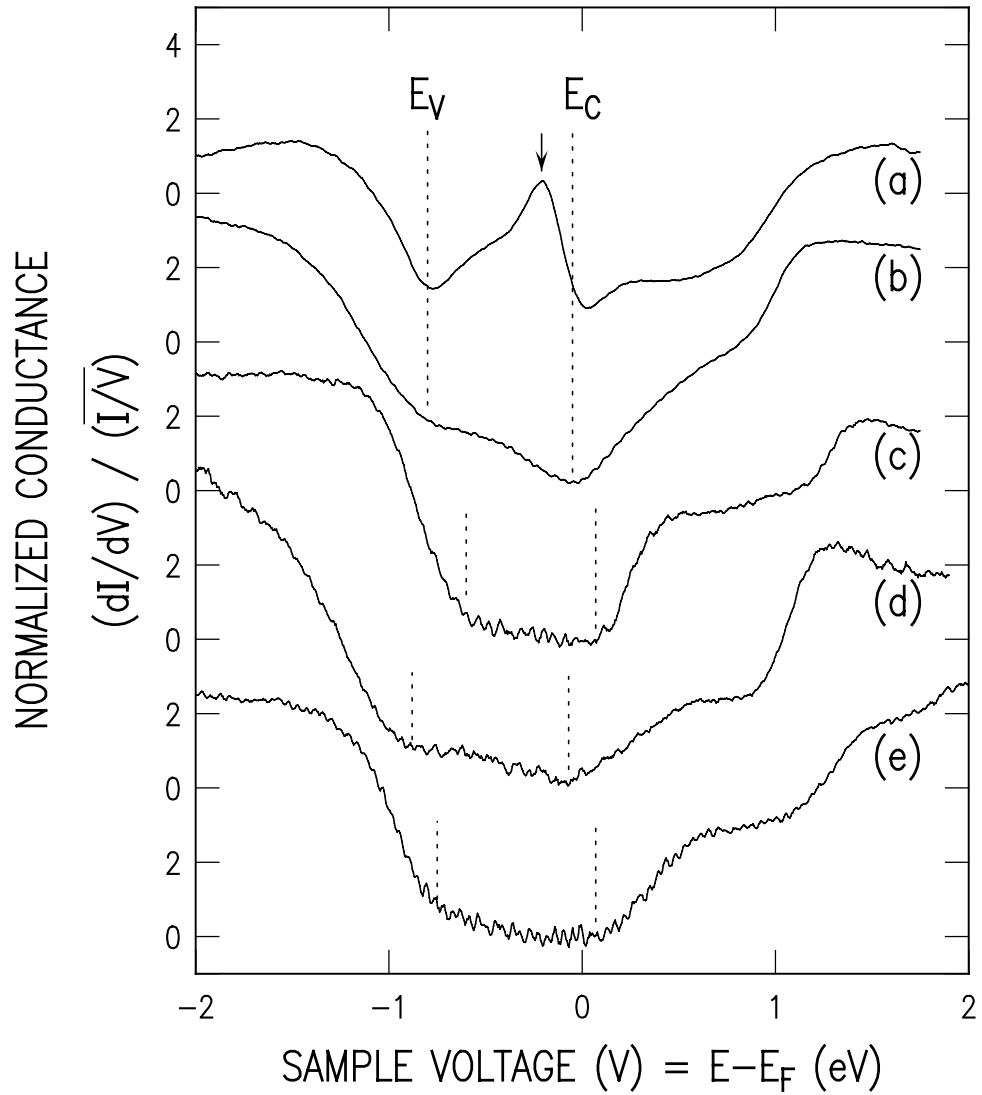


Figure 3 Tunneling spectra (a) and (b) acquired from the undoped LTG-InGaAs layers, (c) from the Be-doped LTG-InGaAs layer, (d) from the annealed undoped LTG-InGaAs layer, and (e) from the annealed Be-doped LTG-InGaAs layer. The valence band maximum (E_V) and conduction band minimum (E_C) are indicated by dashed lines in each spectrum. Spectrum (a) was measured on point defects and reveals a band of midgap states, as indicated by the arrow.